

Article

# Conformational Dependence of the First Hyperpolarizability of the $\text{Li@B}_{10}\text{H}_{14}$ in Solution

Idney Brandão , Tertius L. Fonseca , Herbert C. Georg, Marcos A. Castro and Renato B. Pontes 

Instituto de Física, Universidade Federal de Goiás, Goiânia 74690-900, GO, Brazil

\* Correspondence: tertius@ufg.br

**Abstract:** Using the ASEC-FEG approach in combination with atomistic simulations, we performed geometry optimizations of a  $C_s$  conformer of the lithium decahydroborate ( $\text{Li@B}_{10}\text{H}_{14}$ ) complex in chloroform and in water, which has been shown to be the most stable in the gas phase and calculated its first hyperpolarizability. At room temperature, ASEC-FEG calculations show that this conformer is stable only in chloroform. However, it is found that the nonlinear response of the  $C_s$  conformer in chloroform is mild, and the result for the hyperpolarizability is markedly decreased in comparison with the result of the  $C_{2v}$  conformer.

**Keywords:** atomistic simulation; hyperpolarizability; electrides; polar solvents

## 1. Introduction

Among the molecular systems with nonlinear optical (NLO) responses, electrides have excess electrons that are not located on any specific atom [1,2]. Several theoretical investigations have demonstrated that electride-like structures can be designed by doping an alkali metal atom into organic complexants and can exhibit extraordinary NLO properties relative to the corresponding undoped organic ones [3–11]. However, organic electrides may have limited practical applications due to their thermal instability at room temperature and reactivity with air [1,12].

Electrides with relatively good thermal stability and NLO properties have been designed by the addition of lithium atoms to inorganic borane clusters [13–15]. In particular, Muhammad et al. [13] showed, in the gas phase, that an inorganic electride obtained from adding a Li atom to the cavity of decaborane ( $\text{B}_{10}\text{H}_{14}$ ) can have a remarkable first hyperpolarizability. In that study, the authors considered an arrangement in which an added Li atom interacts with terminal H atoms on the open face of the basket-shaped molecule ( $C_{2v}$  symmetry). Based on this geometric structure, we carried out an investigation of the stability of this molecular shape of  $\text{Li@B}_{10}\text{H}_{14}$  in chloroform and water. We showed, at room temperature, that the geometric changes induced in solution in the  $C_{2v}$  conformer of  $\text{Li@B}_{10}\text{H}_{14}$  result in a stable structure only in chloroform [16]. Recently, Medved et al. [17] have shown, in the gas phase, based on the global energy minimum analysis, that  $C_s$  conformers (Li atoms close to the decaborane basket from the side or the side-bottom) of  $\text{Li@B}_{10}\text{H}_{14}$  can be significantly more stable than the  $C_{2v}$  structure, with possible consequences on their NLO responses. Thus, from the most recent theoretical results, there is a possibility that  $\text{Li@B}_{10}\text{H}_{14}$  conformers containing a loosely bound excess electron may be stable in the solution and present different NLO responses.

In the present study, we report the results on the stability and first hyperpolarizability of a  $C_s$  conformer of  $\text{Li@B}_{10}\text{H}_{14}$  (Figure 1) in chloroform and water solvents, which has been shown to be the most stable in the gas phase [17]. This represents an extension of a previous calculation on the stability and first hyperpolarizability of the  $C_{2v}$  conformer of  $\text{Li@B}_{10}\text{H}_{14}$  (Figure 1) in solution [16]. The absorption spectrum is also presented, considering that the addition of an excess electron can affect the electronic excitation energies of this inorganic electride. The equilibrium structure of the  $C_s$  conformer in each medium, at



**Citation:** Brandão, I.; Fonseca, T.L.; Georg, H.C.; Castro, M.A.; Pontes, R.B. Conformational Dependence of the First Hyperpolarizability of the  $\text{Li@B}_{10}\text{H}_{14}$  in Solution. *Liquids* **2023**, *3*, 159–167. <https://doi.org/10.3390/liquids3010012>

Academic Editor: Enrico Bodo

Received: 26 November 2022

Revised: 13 January 2023

Accepted: 15 February 2023

Published: 20 February 2023



**Copyright:** © 2023 by the authors. Licensee MDPI, Basel, Switzerland. This article is an open access article distributed under the terms and conditions of the Creative Commons Attribution (CC BY) license (<https://creativecommons.org/licenses/by/4.0/>).

temperature and pressure under ambient conditions, was obtained using the ASEC-FEG scheme [18–25] by employing iteratively the sequential quantum mechanics/molecular mechanics (S-QM/MM) method [26,27]. The S-QM/MM approach has been successfully applied to reliably describe the effects of solvent on the electronic properties of solute molecules [28–32].

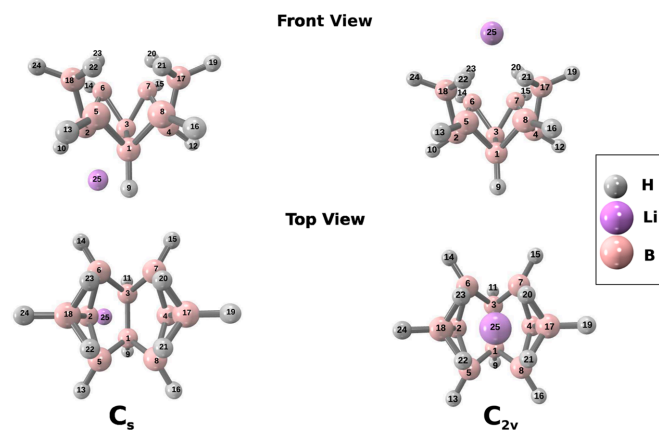


**Figure 1.** Stable conformers of Li@B<sub>10</sub>H<sub>14</sub> (left, C<sub>s</sub> conformer and right, C<sub>2v</sub> conformer).

## 2. Computational Details

We have used the ASEC-FEG methodology to optimize the geometry of the Li@B<sub>10</sub>H<sub>14</sub> system in the solution. The methodology is described in detail in previous papers [22–25]. Briefly, it consists in applying iteratively the Sequential QM/MM methodology [26,27] combined with the Average Solvent Electrostatic Configuration (ASEC) mean field technique [21] and the Free Energy Gradient (FEG) method [18–20] to provide free energy gradients and Hessians to feed a quasi-Newton optimization procedure in the search for the nearest local minimum in the free energy hypersurface.

During the classical simulations, all solvent molecules were kept rigid, and the temperature and pressure were kept at ambient conditions. The molecular properties of the solution were obtained with the unrestricted second-order Møller–Plesset Perturbation Theory (UMP2) using the ASEC mean field [21], where the solvent molecules were treated as point charges. Following previous work [16], boron and hydrogen atoms were described with the cc-pVDZ basis set. For the lithium atom, the aug-cc-pVDZ basis set was used because it is more appropriate to describe the loosely bound valence electron. Thus, for the ASEC-FEG geometry optimizations of the C<sub>s</sub> conformer of Li@B<sub>10</sub>H<sub>14</sub>, such basis sets were used, denoted as (Li-aug)-cc-pVDZ. For water, the potential used was the extended simple point charge (SPC/E) model [33], because it leads to very good agreement for the critical point of water [34]. For chloroform, we have used the OPLS force field [35]. The atomic charges were obtained by performing an electrostatic potential fit (Merz-Kollman) [36] to the MP2/aug-cc-pVDZ charge density.

Here we report the permanent dipole moment ( $\mu$ ) and the first hyperpolarizability properties that can be compared with experimental results of hyper-Rayleigh scattering (HRS) in the solution [37]. The static first hyperpolarizability components ( $\beta_{ijk}$ ) were obtained as numerical differentiation of the energy calculated in the presence of different values of the applied electric field, as implemented in the Gaussian 16 package [38]. Both  $\mu$  and  $\beta_{ijk}$  were calculated at the MP2/aug-cc-pVDZ level of theory. The choice of this basis set is supported by previous tests and ensures a good compromise between computational cost and accuracy [39–41].

In solution, the NLO quantities that can be compared with HRS measurements are the HRS first hyperpolarizability ( $\beta_{\text{HRS}}$ ) and the associated depolarization ratio (DR), given respectively by:

$$\beta_{\text{HRS}} = \sqrt{\langle \beta_{ZZZ}^2 \rangle + \langle \beta_{ZXX}^2 \rangle} \quad (1)$$

and

$$DR = \frac{\langle \beta_{ZZZ}^2 \rangle}{\langle \beta_{ZXX}^2 \rangle}, \quad (2)$$

whose expressions for  $\langle \beta_{ZZZ}^2 \rangle$  and  $\langle \beta_{ZXX}^2 \rangle$  are given in Ref. [42].

The vertical electronic excitation energies were calculated using the TD-DFT method with different exchange–correlation functionals based on the generalized gradient approximation (GGA): LC-BLYP [43], CAM-B3LYP [44], M05-2X [45], and M06-2X [46] functionals. The aug-cc-pVDZ basis has been adopted in all TD-DFT calculations. All QM calculations were performed using unrestricted methods, and the spin contamination was found to be very small, less than 2% from the exact expected value. The classical Monte Carlo simulations were performed with the DICE program [47] and the QM calculations with the Gaussian 16 program [38].

### 3. Results and Discussion

Table 1 shows the MP2/(Li-aug)-cc-pVDZ results for bond lengths between the Li atom and closest B and H atoms of the optimized geometry of  $C_s$  conformer of  $Li@B_{10}H_{14}$  in the gas phase, chloroform, and water. The converged values of maximum and RMS forces are below  $6.5 \times 10^{-4}$  and  $2.5 \times 10^{-4}$  hartree/bohr, respectively, which are reasonable values considering fluctuations due to liquid dynamics [22]. For the  $C_s$  conformer in chloroform, there is a slight increase in the bond lengths  $B_1$ –Li,  $B_2$ –Li, and  $B_3$ –Li relative to the gas phase results, but these are smaller than the corresponding closest distances of the  $C_{2v}$  conformer [16]. This indicates that the  $C_s$  conformer of  $Li@B_{10}H_{14}$  is stable at room temperature in chloroform. Differently, the electrone-like structure of the  $C_s$  conformer is unstable in water at room temperature, and during the simulations, the lithium ion dissociates, as previously shown for the  $C_{2v}$  conformer [16]. Nevertheless, we compute the properties of interest using the *in-water* geometry from the last step of the iterative process.

**Table 1.** MP2/(Li-aug)-cc-pVDZ results for bond lengths (Å) of the  $C_s$  conformer in the gas phase and solution. In the case of chloroform, the values are convergent within an error bar of 0.001 Å.

Length	Gas-Phase	Chloroform (Converged Value)	Water (Last Step Value)
B1-Li	2.256	2.295	3.150
B2-Li	2.244	2.281	3.230
B3-Li	2.256	2.295	3.228
H9-Li	2.021	2.051	2.679
H10-Li	1.957	1.980	2.764
H11-Li	2.021	2.051	2.981
H23-Li	2.043	2.169	2.819

Having obtained the optimized geometry of the  $C_s$  conformer in chloroform, the relative stability of the  $C_s$  and  $C_{2v}$  conformers is evaluated at the MP2/aug-cc-pVDZ level. Our energy calculations indicate that the  $C_s$  conformer in chloroform is more stable than the  $C_{2v}$  conformer by an amount of 21 kcal/mol. This finding is in agreement with the previous study by Medved et al. [17], which showed that the  $C_s$  conformer is the most stable form of  $Li@B_{10}H_{14}$  in the gas phase. It should be emphasized that the inclusion of the solute-solvent interaction contribution in the energy calculations of the conformers gives a marked decrease in the energy difference between the conformers, which is 35 kcal/mol in the gas phase. Following previous work [16], we have also calculated the vertical ionization potential (VIP) of the  $C_s$  conformer in the gas phase and solution at the MP2/aug-cc-pVDZ level, used as an indicator of thermal stability. It is found that the

formation of excess electrons is slightly more stable in chloroform (6.27 eV) than in the gas phase (6.06 eV). In chloroform, however, our previous result indicated that the excess electron is slightly more stable for the  $C_{2v}$  conformer (6.66 eV) [16] than for the  $C_s$  one. In water, the VIP value of 6.05 eV for the  $C_s$  conformer also suggests relative stability for the excess electron on the decaborane cluster. For comparison, the VIP value for the  $C_s$  conformer in chloroform is significantly larger than some electriles formed by doping the lithium atom in organic compounds, such as Li@calyx[4]pyrrole (4.16 eV) [3], Li-[15]aneN<sub>5</sub> (2.32 eV) [6], and (Li<sup>+</sup>@n<sup>6</sup>adz)Li<sup>-</sup> (2.88 eV) [48].

Figure 2 illustrates the behavior of the dipole moment of the  $C_s$  conformer in chloroform solution during the iterative process, indicating a rapid convergence pattern. The MP2/aug-cc-pVDZ results for  $\mu$  of the  $C_s$  conformer in the gas phase and solution are quoted in Table 2. The corresponding results for the  $C_{2v}$  conformer are also reported in this table. For the  $C_s$  conformer in chloroform, partial negative charges are distributed on the boron and hydrogen atoms closest to the lithium atom, and the polarization effect induces a slight increase in  $q(\text{Li})$ , with the *in*-chloroform value of 0.81  $e$  when compared with the gas phase result of 0.77  $e$ . This leads to the *in*-chloroform result for  $\mu$  of 2.91 a.u., which is increased by 15% when compared to the gas phase result of 2.53 a.u., but it is 37% smaller than the *in*-chloroform result for the  $C_{2v}$  conformer of 4.59 a.u. [16]. In water, the excess charge of the  $C_s$  conformer is delocalized over the decaborane cluster. The *in*-water  $q(\text{Li})$  charge is found to be 0.97  $e$ , close to +1  $e$ , which shows that the Li atom has been ionized to form a cation and the B<sub>10</sub>H<sub>14</sub> anion, and the *in*-water  $\mu$  value is increased by 59% relative to the gas phase value. In the gas phase, our MP2/aug-cc-pVDZ results for  $\mu$  are in good agreement with the MP2/6-31+G(d)/MP2/aug-cc-pVDZ results of Medved et al. [17], which are also quoted in Table 2, whose differences do not reach 4%.

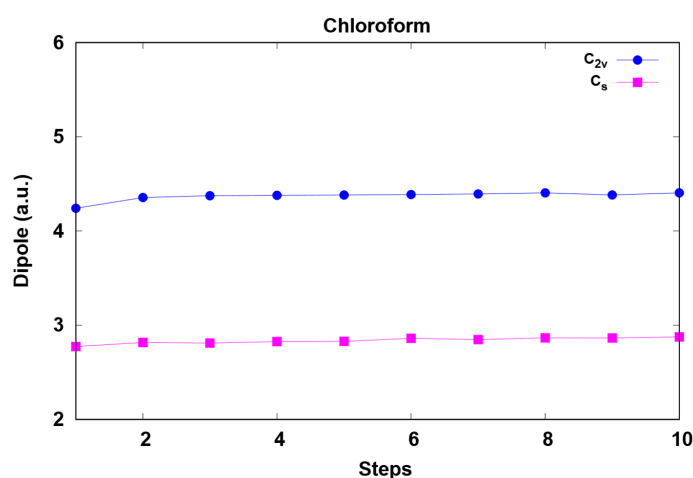


**Figure 2.** Behavior of the dipole moment of the  $C_s$  conformer in chloroform during the iterative process. For comparison, the corresponding results for the  $C_{2v}$  conformer (taken from Ref. [16]) are included.

**Table 2.** MP2/aug-cc-pVDZ results for the dipole moment (in a.u.) of the  $C_s$  conformer in the gas phase and solution. For comparison, the corresponding results for the  $C_s$  and  $C_{2v}$  conformers are included.

Conformer	Gas-Phase	Chloroform (Converged Value)	Water (Last Step Value)
$C_s$	2.53 (2.55 <sup>2</sup> )	2.91	6.56
$C_{2v}$	3.59 <sup>1</sup> (3.72 <sup>2</sup> )	4.59 <sup>1</sup>	9.42 <sup>1</sup>

<sup>1</sup> Results taken from Ref. [16]. <sup>2</sup> Results taken from Ref. [17].

MP2/aug-cc-pVDZ results for the static HRS first hyperpolarizability and depolarization ratio of the  $C_s$  conformer obtained in the gas phase and solution are gathered in Table 3. The corresponding results for the  $C_{2v}$  conformer are also reported in this table. One can see that the polarization effect of the excess electron for  $\beta_{HRS}$  of the  $Li@B_{10}H_{14}$  complex is particularly affected by the conformational structure, as shown by Medved et al. [17]. In the gas phase, the result for  $\beta_{HRS}$  of the  $C_s$  conformer (504 a.u.) is markedly reduced by 92% when compared with that of the  $C_{2v}$  conformer (6214 a.u.). As shown in previous work [16], however, the electrone-like characteristic gives a very large hyperpolarizability for the  $C_{2v}$  conformer.

**Table 3.** MP2/aug-cc-pVDZ results for the static HRS first hyperpolarizability (in a.u.) and depolarization ratio of the  $C_s$  conformer. For comparison, the corresponding results for the  $C_{2v}$  conformer are included.

Conformer	$\beta_{HRS}$ (a.u.)			DR		
	Gas-Phase	Chloroform (Converged Value)	Water (Last Step Value)	Gas-Phase	Chloroform (Converged Value)	Water (Last Step Value)
$C_s$	504	212	154	4.94	4.02	7.23
$C_{2v}$ <sup>1</sup>	6214	2786	64	6.20	6.52	3.57

<sup>1</sup> Results taken from Ref. [16].

Our MP2/aug-cc-pVDZ results for  $\beta_{HRS}$  of the  $C_s$  conformer are very sensitive to the solvent effects, with significant reductions in chloroform and in water. For this conformer in chloroform, the result of 212 a.u. for  $\beta_{HRS}$  has a significant decrease (58%) relative to the gas phase result of 504 a.u., indicating that the contribution of the excess electron for  $\beta_{HRS}$  is mild. In water, the MP2 model predicts for  $\beta_{HRS}$  of the  $C_s$  conformer a result of 154 a.u. which is 27% smaller than the result in chloroform. Despite the structure of the  $C_s$  conformer being unstable in water, the first hyperpolarizability is not significantly affected in relation to the value in chloroform. Notice that solvent effects significantly impact the depolarization ratio (Table 3) of the  $C_s$  conformer in water, and the DR value of 7.23 indicates a marked dipolar contribution to  $\beta_{HRS}$ . In chloroform, however, there is a less pronounced dipolar contribution to  $\beta_{HRS}$ , whose DR value of 4.02 for the  $C_s$  conformer is 38% smaller than the corresponding value of the  $C_{2v}$  conformer.

A qualitative interpretation of the solvent dependence of the hyperpolarizability of the  $C_s$  conformer can be obtained from the two-level model [49], where  $\beta_{HRS}$  is proportional to the difference between the crucial excited state permanent dipole moment and the ground state permanent dipole moment ( $\Delta\mu$ ) and the oscillator strength ( $f_0$ ) and inversely proportional to the third power of the transition energy ( $\Delta E$ ):

$$\beta_{HRS} \propto \Delta\mu f_0 / \Delta E^3 \quad (3)$$

In this model, the transition energy plays an important role in determining the first hyperpolarizability. For the  $C_s$  conformer, the first absorption band is dominated by a highest occupied orbital molecular (HOMO)  $\rightarrow$  lowest unoccupied orbital molecular (LUMO) excitation. However, TD-DFT results indicate that the first transition has a very small oscillator strength, regardless of the environment.

Figure 3 shows the absorption spectra of the  $C_s$  conformer in the gas phase and the solution obtained at the CAM-B3LYP/aug-cc-pVDZ level. The corresponding spectra for the  $C_{2v}$  conformer are also reported in this figure. TD-DFT/aug-cc-pVDZ results for the excitation energy and oscillator strength of the more intense electronic transition of the  $C_s$  conformer are quoted in Table 4. The corresponding results for the first electronic transition  $C_{2v}$  conformer are also reported in this table. One can see that the absorption spectra of the  $C_s$  conformer, not only in chloroform but also in water, are characterized by more intense transitions with energies larger than 4 eV. Thus, there is a considerable

difference between the crucial electronic transition energies for  $C_s$  and  $C_{2v}$  conformers in both chloroform and water by a factor around 2, and, therefore, the main factor for the marked decrease of  $\beta_{HRS}$  of the  $C_s$  conformer is related to the significant increases of the crucial transition energy (Equation (3)). In addition, similar energy values for the more intense transition in chloroform and water, suggest that the  $\beta_{HRS}$  of the  $C_s$  conformer does not change significantly in any environment.

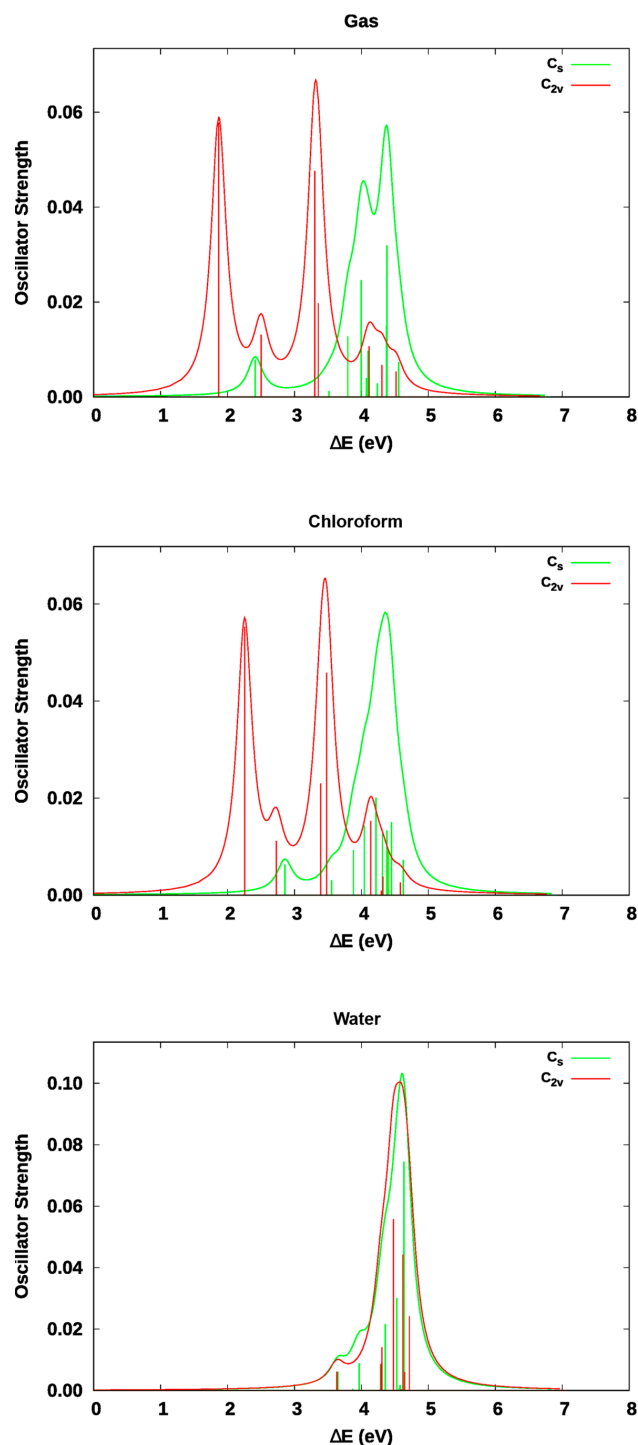


**Figure 3.** Absorption spectra of the  $C_s$  conformer in the gas phase and solution. For comparison, the corresponding results for the  $C_{2v}$  conformer (taken from Ref. [16]) are included.

**Table 4.** TD-DFT results for excitation energy (in eV) and (oscillator strength) of the more intense electronic transition (considering the first 10 excited states) of the  $C_s$  conformer in gas phase and in solution. For comparison, the results for the first electronic transition of the  $C_{2v}$  conformer are included. All results were obtained using the aug-cc-pVDZ basis set.

Method	$C_s$ Conformer			$C_{2v}$ Conformer <sup>1</sup>		
	Gas-Phase	Chloroform (Converged Value)	Water (Last Step Value)	Gas-Phase	Chloroform (Converged Value)	Water (Last Step Value)
LC-BLYP	4.58 (0.0302)	4.48 (0.0439)	4.90 (0.0723)	2.23 (0.0504)	2.59 (0.0505)	3.81 (0.0069)
M05-2X	4.10 (0.0300)	4.21 (0.0331)	4.58 (0.0773)	2.28 (0.0503)	2.64 (0.0494)	3.55 (0.0065)
M06-2X	3.65 (0.0211)	3.95 (0.0225)	4.30 (0.0351)	1.92 (0.0573)	2.43 (0.0522)	3.44 (0.0011)
CAM-B3LYP	4.38 (0.0319)	4.22 (0.0201)	4.64 (0.0744)	1.87 (0.0578)	2.25 (0.0553)	3.63 (0.0061)

<sup>1</sup> Results taken from Ref. [16].

#### 4. Conclusions

We have more recently shown that the  $C_{2v}$  conformer of the  $Li@B_{10}H_{14}$  complex, which had its NLO properties studied in the gas phase by Muhammad et al., is a stable structure in chloroform at room temperature. However, Medved et al. have recently shown that  $C_s$  conformers of the  $Li@B_{10}H_{14}$  complex in the gas phase can be significantly more stable than the  $C_{2v}$  conformer, with a marked effect on the second-order NLO properties. In this work, we report an investigation on the stability and first hyperpolarizability of a  $C_s$  conformer in aprotic and protic solvents using the sequential QM/MM methodology in combination with the ASEC-FEG model, which has been shown to be the most stable in the gas phase. ASEC-FEG calculations show that the solvent-induced geometric changes in the  $C_s$  conformer at room temperature result in a stable structure in chloroform and an unstable structure in water. Our MP2 results show that the  $C_s$  conformer in chloroform is more stable than the  $C_{2v}$  conformer by an amount of 21 kcal/mol, which confirms the finding of Medved et al. However, the relative stability of the conformers is significantly reduced due to the solute-solvent interaction energy when compared with the gas phase result, which is 35 kcal/mol. Polarization effects due to the electrostatic embedding lead to a reduction of 58% of the hyperpolarizability of the  $C_s$  conformer in chloroform in comparison with the gas result of 504 a.u. In chloroform, the contribution of the excess electron to the first hyperpolarizability of the  $C_s$  conformer is mild, and the result for  $\beta_{HRS}$  of 212 a.u. is markedly decreased by a factor of 92% in comparison with the corresponding result for the  $C_{2v}$  conformer of 2786 a.u. Therefore, the small first hyperpolarizability of the  $C_s$  conformer suggests that this inorganic electride-type system should not present significant second-order nonlinear responses in any environment. This finding also illustrates that the influence of the environment must be carefully considered in the design of new molecules with excess electrons that are stable at room temperature for aiming applications in NLO.

**Author Contributions:** I.B.: data curation, formal analysis, writing—review and editing. T.L.F.: conceptualization, formal analysis, writing—original draft, writing—review and editing. H.C.G.: data curation, formal analysis, writing—review and editing. M.A.C.: formal analysis, writing—review and editing. R.B.P.: formal analysis, writing—review and editing. All authors have read and agreed to the published version of the manuscript.

**Funding:** This research received no external funding.

**Data Availability Statement:** Data are contained within the article and bibliography.

**Acknowledgments:** The authors gratefully acknowledge the financial support of CNPq, CAPES, and FAPEG (PRONEX) agencies (Brazil) as well as the computer resources of the LaMCAD/UFG laboratory.

**Conflicts of Interest:** The authors declare no conflict of interest.

## References

1. Dye, J.L. Electrons as Anions. *Science* **2003**, *301*, 607–608. [[CrossRef](#)]
2. Dye, J.L. Electrides: Early Examples of Quantum Confinement. *Acc. Chem. Res.* **2009**, *42*, 1564–1572. [[CrossRef](#)]
3. Chen, W.; Li, Z.R.; Wu, D.; Li, Y.; Sun, C.C.; Gu, F.L. The Structure and the Large Nonlinear Optical Properties of Li@calix[4]Pyrrole. *J. Am. Chem. Soc.* **2005**, *127*, 10977–10981. [[CrossRef](#)] [[PubMed](#)]
4. Chen, W.; Li, Z.R.; Wu, D.; Li, R.Y.; Sun, C.C. Theoretical Investigation of the Large Nonlinear Optical Properties of (HCN)<sub>n</sub> Clusters with Li Atom. *J. Phys. Chem. B* **2005**, *109*, 601–608. [[CrossRef](#)] [[PubMed](#)]
5. Xu, H.L.; Li, Z.R.; Wu, D.; Wang, B.Q.; Li, Y.; Gu, F.L.; Aoki, Y. Structures and Large NLO Responses of New Electrides: Li-Doped Fluorocarbon Chain. *J. Am. Chem. Soc.* **2007**, *129*, 2967–2970. [[CrossRef](#)] [[PubMed](#)]
6. Li, Z.J.; Li, Z.R.; Wang, F.F.; Luo, C.; Ma, F.; Wu, D.; Wang, Q.; Huang, X.R. A Dependence on the Petal Number of the Static and Dynamic First Hyperpolarizability for Electride Molecules: Many-Petal-Shaped Li-Doped Cyclic Polyamines. *J. Phys. Chem. A* **2009**, *113*, 2961–2966. [[CrossRef](#)] [[PubMed](#)]
7. Xu, H.-L.; Li, Z.R.; Wu, D.; Ma, F.; Li, Z.J.; Gu, F.L. Lithiation and Li-Doped Effects of [5]Cyclacene on the Static First Hyperpolarizability. *J. Phys. Chem. C* **2009**, *113*, 4984–4986. [[CrossRef](#)]
8. Liu, Z.B.; Zhou, Z.J.; Li, Y.; Li, Z.R.; Wang, R.; Li, Q.Z.; Li, Y.; Jia, F.Y.; Wang, Y.F.; Li, Z.J.; et al. Push-Pull Electron Effects of the Complexant in a Li Atom Doped Molecule with Electride Character: A New Strategy to Enhance the First Hyperpolarizability. *Phys. Chem. Chem. Phys.* **2010**, *12*, 10562–10568. [[CrossRef](#)]
9. Xu, H.L.; Sun, S.L.; Muhammad, S.; Su, Z.M. Three-Propeller-Blade-Shaped Electride: Remarkable Alkali-Metal-Doped Effect on the First Hyperpolarizability. *Theor. Chem. Acc.* **2011**, *128*, 241–248. [[CrossRef](#)]
10. Zhong, R.L.; Xu, H.L.; Li, Z.R.; Su, Z.M. Role of Excess Electrons in Nonlinear Optical Response. *J. Phys. Chem. Lett.* **2015**, *6*, 612–619. [[CrossRef](#)]
11. Oliveira, I.M.; Castro, M.A.; Leão, S.A.; Fonseca, T.L.; Pontes, R.B. Li<sub>4</sub>C<sub>4</sub>H<sub>2</sub>N<sub>2</sub>: A Molecule with Large Hyperpolarizabilities and Electride Characteristic. *Int. J. Quantum Chem.* **2018**, *118*, e25661. [[CrossRef](#)]
12. Matsushita, S.; Toda, Y.; Miyakawa, M.; Hayashi, K.; Kamiya, T.; Hirano, M.; Tanaka, I.; Hosono, H. High-Density Electron Anions in a Nanoporous Single Crystal: [Ca<sub>24</sub>Al<sub>28</sub>O<sub>64</sub>]<sup>4+</sup> (4e<sup>-</sup>). *Science* **2003**, *301*, 626–629. [[CrossRef](#)] [[PubMed](#)]
13. Muhammad, S.; Xu, H.; Liao, Y.; Kan, Y.; Su, Z. Quantum Mechanical Design and Structure of the Li@B<sub>10</sub>H<sub>14</sub> Basket with a Remarkably Enhanced Electro-Optical Response. *J. Am. Chem. Soc.* **2009**, *131*, 11833–11840. [[CrossRef](#)]
14. Muhammad, S.; Xu, H.; Su, Z. Capturing a Synergistic Effect of a Conical Push and an Inward Pull in Fluoro Derivatives of Li@B<sub>10</sub>H<sub>14</sub> Basket: Toward a Higher Vertical Ionization Potential and Nonlinear Optical Response. *J. Phys. Chem. A* **2011**, *115*, 923–931. [[CrossRef](#)] [[PubMed](#)]
15. Ma, N.; Gong, J.; Li, S.; Zhang, J.; Qiu, Y.; Zhang, G. Second-Order NLO Responses of Two-Cavity Inorganic Electrides Li: N@B<sub>20</sub>H<sub>26</sub> (n = 1, 2): Evolutions with Increasing Excess Electron Number and Various B-B Connection Sites of B<sub>20</sub>H<sub>26</sub>. *Phys. Chem. Chem. Phys.* **2017**, *19*, 2557–2566. [[CrossRef](#)] [[PubMed](#)]
16. Brandão, I.; Fonseca, T.L.; Georg, H.C.; Castro, M.A.; Pontes, R.B. Assessing the Structure and First Hyperpolarizability of Li@B<sub>10</sub>H<sub>14</sub> in Solution: A Sequential QM/MM Study Using the ASEC-FEG Method. *Phys. Chem. Chem. Phys.* **2020**, *22*, 17314–17324. [[CrossRef](#)]
17. Medved, M.; Demissie, T.B.; McKee, M.L.; Hnyk, D. The Behavior of a Paramagnetic System in Electric and Magnetic Fields as Exemplified by Revisiting Li@B<sub>10</sub>H<sub>14</sub>. *Phys. Chem. Chem. Phys.* **2017**, *19*, 12229–12236. [[CrossRef](#)]
18. Okuyama-Yoshida, N.; Nagaoka, M.; Yamabe, T. Transition-State Optimization on Free Energy Surface: Toward Solution Chemical Reaction Ergodography. *Int. J. Quantum Chem.* **1998**, *70*, 95–103. [[CrossRef](#)]
19. Okuyama-Yoshida, N.; Kataoka, K.; Nagaoka, M.; Yamabe, T. Structure Optimization via Free Energy Gradient Method: Application to Glycine Zwitterion in Aqueous Solution. *J. Chem. Phys.* **2000**, *113*, 3519–3524. [[CrossRef](#)]
20. Hirao, H.; Nagae, Y.; Nagaoka, M. Transition-State Optimization by the Free Energy Gradient Method: Application to Aqueous-Phase Menshutkin Reaction between Ammonia and Methyl Chloride. *Chem. Phys. Lett.* **2001**, *348*, 350–356. [[CrossRef](#)]
21. Coutinho, K.; Georg, H.C.; Fonseca, T.L.; Ludwig, V.; Canuto, S. An Efficient Statistically Converged Average Configuration for Solvent Effects. *Chem. Phys. Lett.* **2007**, *437*, 148–152. [[CrossRef](#)]
22. Georg, H.C.; Canuto, S. Electronic Properties of Water in Liquid Environment: A Sequential QM/MM Study Using the Free Energy Gradient Method. *J. Phys. Chem. B* **2012**, *116*, 11247–11254. [[CrossRef](#)] [[PubMed](#)]
23. Franco, L.R.; Brandão, I.; Fonseca, T.L.; Georg, H.C. Elucidating the Structure of Merocyanine Dyes with the ASEC-FEG Method. Phenol Blue in Solution. *J. Chem. Phys.* **2016**, *145*, 194301. [[CrossRef](#)] [[PubMed](#)]
24. Brandão, I.; Franco, L.R.; Fonseca, T.L.; Castro, M.A.; Georg, H.C. Confirming the Relationship between First Hyperpolarizability and the Bond Length Alternation Coordinate for Merocyanine Dyes. *J. Chem. Phys.* **2017**, *146*, 224505. [[CrossRef](#)] [[PubMed](#)]
25. Valverde, D.; Georg, H.C.; Canuto, S. Free-Energy Landscape of the SN<sub>2</sub> Reaction CH<sub>3</sub>Br + Cl<sup>-</sup> → CH<sub>3</sub>Cl + Br<sup>-</sup> in Different Liquid Environments. *J. Phys. Chem. B* **2022**, *126*, 3685–3692. [[CrossRef](#)] [[PubMed](#)]
26. Coutinho, K.; Canuto, S. Solvent Effects from a Sequential Monte Carlo-Quantum Mechanical Approach. *Adv. Quantum Chem.* **1997**, *28*, 89–105. [[CrossRef](#)]
27. Coutinho, K.; Canuto, S. Solvent Effects in Emission Spectroscopy: A Monte Carlo Quantum Mechanics Study of the n ← π\* Shift of Formaldehyde in Water. *J. Chem. Phys.* **2000**, *113*, 9132–9139. [[CrossRef](#)]

28. Fonseca, T.L.; Coutinho, K.; Canuto, S. Probing Supercritical Water with the  $n-\pi^*$  Transition of Acetone: A Monte Carlo/Quantum Mechanics Study. *J. Chem. Phys.* **2007**, *126*, 034508. [[CrossRef](#)]
29. Fonseca, T.L.; Georg, H.C.; Coutinho, K.; Canuto, S. Polarization and Spectral Shift of Benzophenone in Supercritical Water. *J. Phys. Chem. A* **2009**, *113*, 5112–5118. [[CrossRef](#)]
30. Fonseca, T.L.; Coutinho, K.; Canuto, S. Hydrogen Bond Interactions between Acetone and Supercritical Water. *Phys. Chem. Chem. Phys.* **2010**, *12*, 6660–6665. [[CrossRef](#)]
31. Junior, L.A.; Colherinhas, G.; Fonseca, T.L.; Castro, M.A. Solvent Effects on the First Hyperpolarizability of Retinal Derivatives. *Chem. Phys. Lett.* **2014**, *598*, 43–47. [[CrossRef](#)]
32. Oliveira, L.B.A.; Colherinhas, G.; Fonseca, T.L.; Castro, M.A. Spectroscopic Properties of Vitamin E Models in Solution. *Chem. Phys. Lett.* **2015**, *628*, 49–53. [[CrossRef](#)]
33. Berendsen, H.J.C.; Grigera, J.R.; Straatsma, T.P. The missing term in effective pair potentials. *J. Phys. Chem.* **1987**, *91*, 6269–6271. [[CrossRef](#)]
34. Guissani, Y.; Guillot, B. A computer simulation study of the liquid–vapor coexistence curve of water. *J. Chem. Phys.* **1993**, *98*, 8221–8235. [[CrossRef](#)]
35. McDonald, N.A.; Carlson, H.A.; Jorgensen, W.L. Free energies of solvation in chloroform and water from a linear response approach. *J. Phys. Org. Chem.* **1997**, *10*, 563–576. [[CrossRef](#)]
36. Besler, B.H.; Merz, K.M.; Kollman, P.A. Atomic charges derived from semiempirical methods. *J. Comput. Chem.* **1990**, *11*, 431–439. [[CrossRef](#)]
37. Clays, K.; Persoons, A. Hyper-Rayleigh Scattering in Solution. *Phys. Rev. Lett.* **1991**, *66*, 2980–2983. [[CrossRef](#)] [[PubMed](#)]
38. Frisch, M.J.; Trucks, G.W.; Schlegel, H.B. *GAUSSIAN 16, Revision B.01*; Gaussian, Inc.: Wallingford, CT, USA, 2016.
39. Naves, E.S.; Castro, M.A.; Fonseca, T.L. Dynamic (Hyper)Polarizabilities of the Ozone Molecule: Coupled Cluster Calculations Including Vibrational Corrections. *J. Chem. Phys.* **2011**, *134*, 054315. [[CrossRef](#)]
40. Silveira, O.; Castro, M.A.; Fonseca, T.L. Vibrational Corrections to the First Hyperpolarizability of the Lithium Salt of Pyridazine Li-H3C4N2. *J. Chem. Phys.* **2013**, *138*, 074312. [[CrossRef](#)]
41. Silveira, O.; Castro, M.A.; Leão, S.A.; Fonseca, T.L. Second Hyperpolarizabilities of the Lithium Salt of Pyridazine Li-H3C4N2 and Lithium Salt Electride Li-H3C4N2. *Chem. Phys. Lett.* **2015**, *633*, 241–246. [[CrossRef](#)]
42. Castet, F.; Bogdan, E.; Plaquet, A.; Ducasse, L.; Champagne, B.; Rodriguez, V. Reference Molecules for Nonlinear Optics: A Joint Experimental and Theoretical Investigation. *J. Chem. Phys.* **2012**, *136*, 024506. [[CrossRef](#)]
43. Iikura, H.; Tsuneda, T.; Yanai, T.; Hirao, K. A Long-Range Correction Scheme for Generalized-Gradient-Approximation Exchange Functionals. *J. Chem. Phys.* **2001**, *115*, 3540–3544. [[CrossRef](#)]
44. Yanai, T.; Tew, D.P.; Handy, N.C. A New Hybrid Exchange–Correlation Functional Using the Coulomb-Attenuating Method (CAM-B3LYP). *Chem. Phys. Lett.* **2004**, *393*, 51–57. [[CrossRef](#)]
45. Zhao, Y.; Schultz, N.E.; Truhlar, D.G. Design of Density Functionals by Combining the Method of Constraint Satisfaction with Parametrization for Thermochemistry, Thermochemical Kinetics, and Noncovalent Interactions. *J. Chem. Theory Comput.* **2006**, *2*, 364–382. [[CrossRef](#)]
46. Zhao, Y.; Truhlar, D.G. The M06 Suite of Density Functionals for Main Group Thermochemistry, Thermochemical Kinetics, Noncovalent Interactions, Excited States, and Transition Elements: Two New Functionals and Systematic Testing of Four M06-Class Functionals and 12 Other Function. *Theor. Chem. Acc.* **2008**, *120*, 215–241. [[CrossRef](#)]
47. Cezar, H.M.; Canuto, S.; Coutinho, K. DICE: A Monte Carlo Code for Molecular Simulation Including the Configurational Bias Monte Carlo Method. *J. Chem. Inf. Model.* **2020**, *60*, 3472–3488. [[CrossRef](#)]
48. Wang, F.F.; Li, Z.R.; Wu, D.; Wang, B.Q.; Li, Y.; Li, Z.J.; Chen, W.; Yu, G.T.; Gu, F.L.; Aoki, Y. Structures and Considerable Static First Hyperpolarizabilities: New Organic Alkalides  $(M^+@n6adz)M'$ - ( $M, M' = Li, Na, K; n = 2, 3$ ) with Cation inside and Anion Outside of the Cage Complexants. *J. Phys. Chem. B* **2008**, *112*, 1090–1094. [[CrossRef](#)]
49. Oudar, J.L.; Chemla, D.S.; Batifol, E. Optical Nonlinearities of Various Substituted Benzene Molecules in the Liquid State, and Comparison with Solid State Nonlinear Susceptibilities. *J. Chem. Phys.* **1977**, *67*, 1626–1635. [[CrossRef](#)]

**Disclaimer/Publisher's Note:** The statements, opinions and data contained in all publications are solely those of the individual author(s) and contributor(s) and not of MDPI and/or the editor(s). MDPI and/or the editor(s) disclaim responsibility for any injury to people or property resulting from any ideas, methods, instructions or products referred to in the content.